

Revisiting the Circumnuclear X-Ray Emission of NGC 2992 in a Historically Low State

Junfeng Wang & Xiaoyu Xu
(Xiamen University)



Abstract

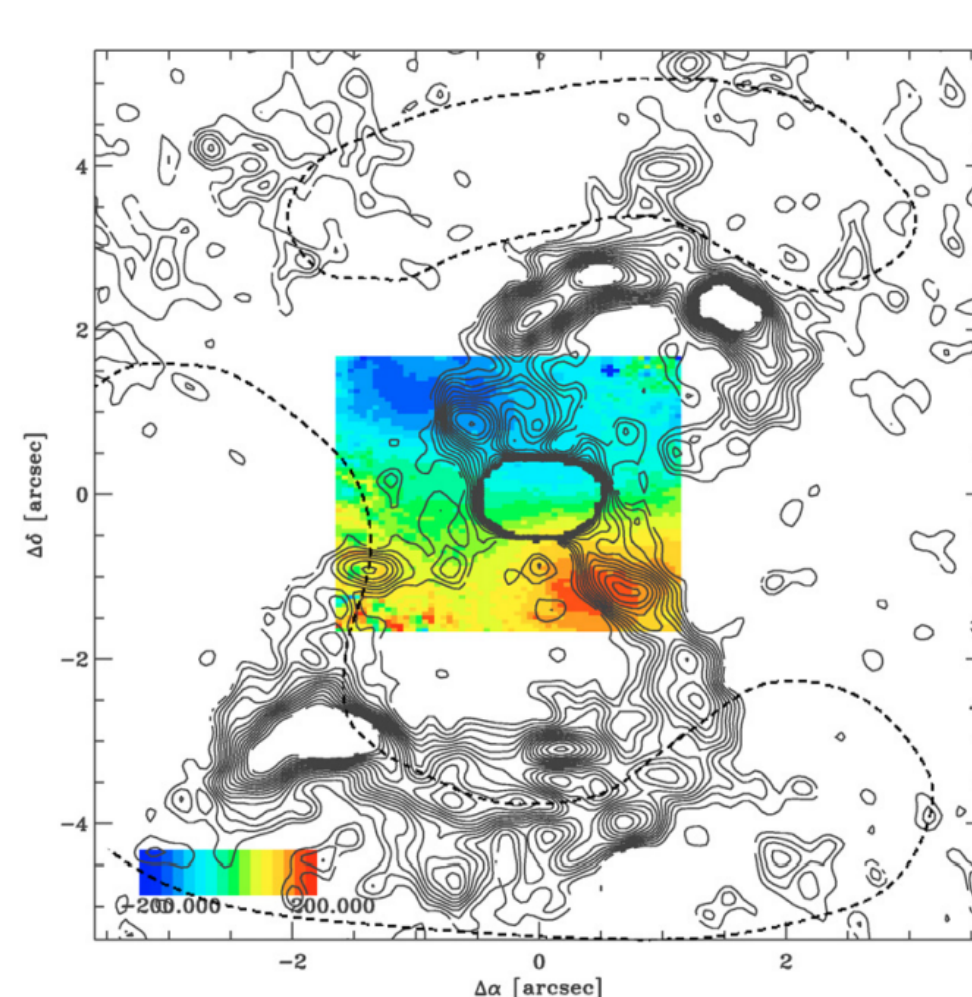
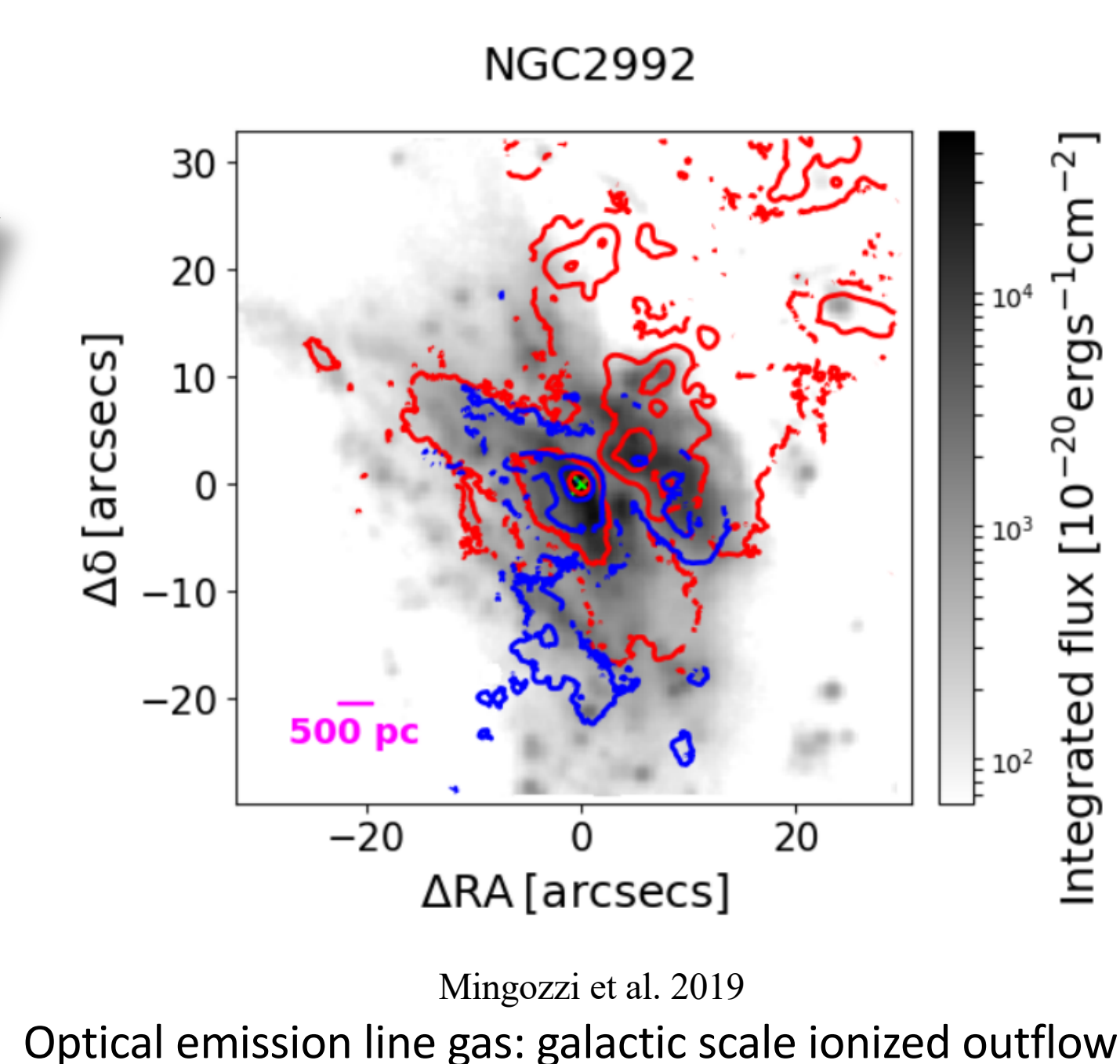
The innermost region of the Seyfert galaxy NGC 2992 has long been suspected to be the location of intense AGN–host galaxy interaction, but photon pile up in previous high-resolution observations hampered the soft X-ray study near its nucleus. We present an X-ray imaging and spectroscopic analysis of the circumnuclear (1''–3'') region of NGC 2992 using the zeroth-order image of a 135 ks Chandra grating observation, which captured the nucleus in a historically low flux state. Extended soft X-ray emission is detected in the circumnuclear region with $L_X \sim 7 \times 10^{39} \text{ erg s}^{-1}$. The majority of the previous detection of soft X-ray excess could be associated with the outflow. An anomalous narrow emission line with a centroid energy of $\sim 4.97 \text{ keV}$ is found. If attributed to *redshifted* highly ionized iron emission (e.g., Fe xxv), the required outflow velocity is $\sim 0.23 c$. We also find extended, asymmetric Fe K α emission along the galactic disk, which could originate from reflection by cold gas on $\sim 200 \text{ pc}$ scale.

Introduction

NGC 2992



Credit: Caelum-Observatory Block (2011)



a nearly edge-on spiral galaxy at $z = 0.00771$ which corresponds to a distance of 32.5 Mpc ($1'' \sim 150 \text{ pc}$). $M_{\text{BH}} \sim 5.2 \times 10^7 M_{\odot}$

Classification is Seyfert 1.9/1.5.

NGC 2992/2993 (Arp245) : the first X-ray detection of NGC 2992 was in 1977 by HEAO-1 at a flux level of about $8 \times 10^{-11} \text{ erg cm}^{-2} \text{ s}^{-1}$

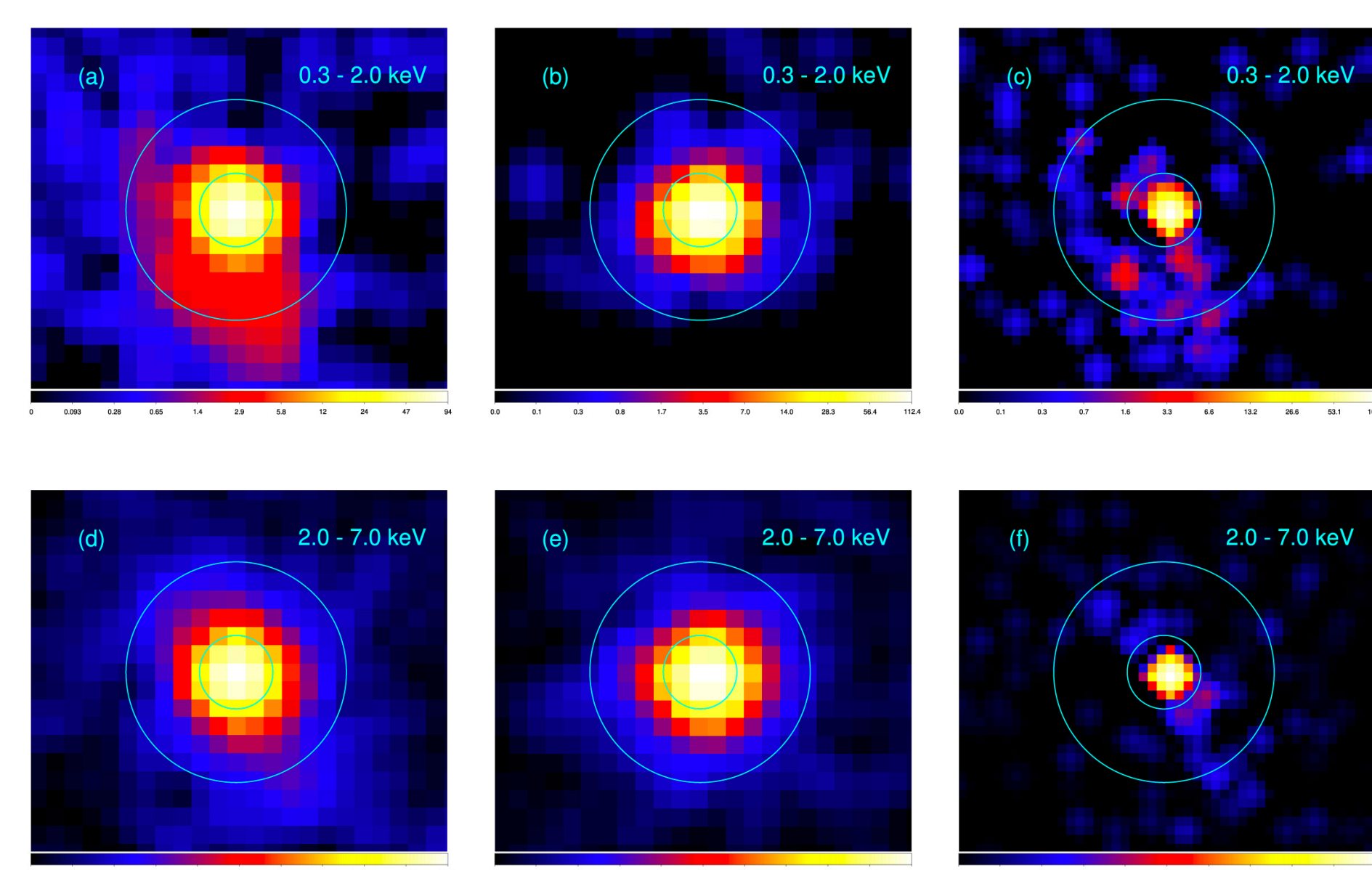
NGC 2992 has two prominent, diffuse, figure-eight-shaped radio bubbles to the northwest and southeast, which have a size of about $8''$

Previous work by Murphy et al. (2017) analyzed these data thoroughly to obtain first-order HEG/MEG spectra.

the 2–10 keV flux of NGC 2992 can vary by a factor of ~ 30 , where the lowest 2–10 keV flux $3 \times 10^{-12} \text{ erg cm}^{-2} \text{ s}^{-1}$

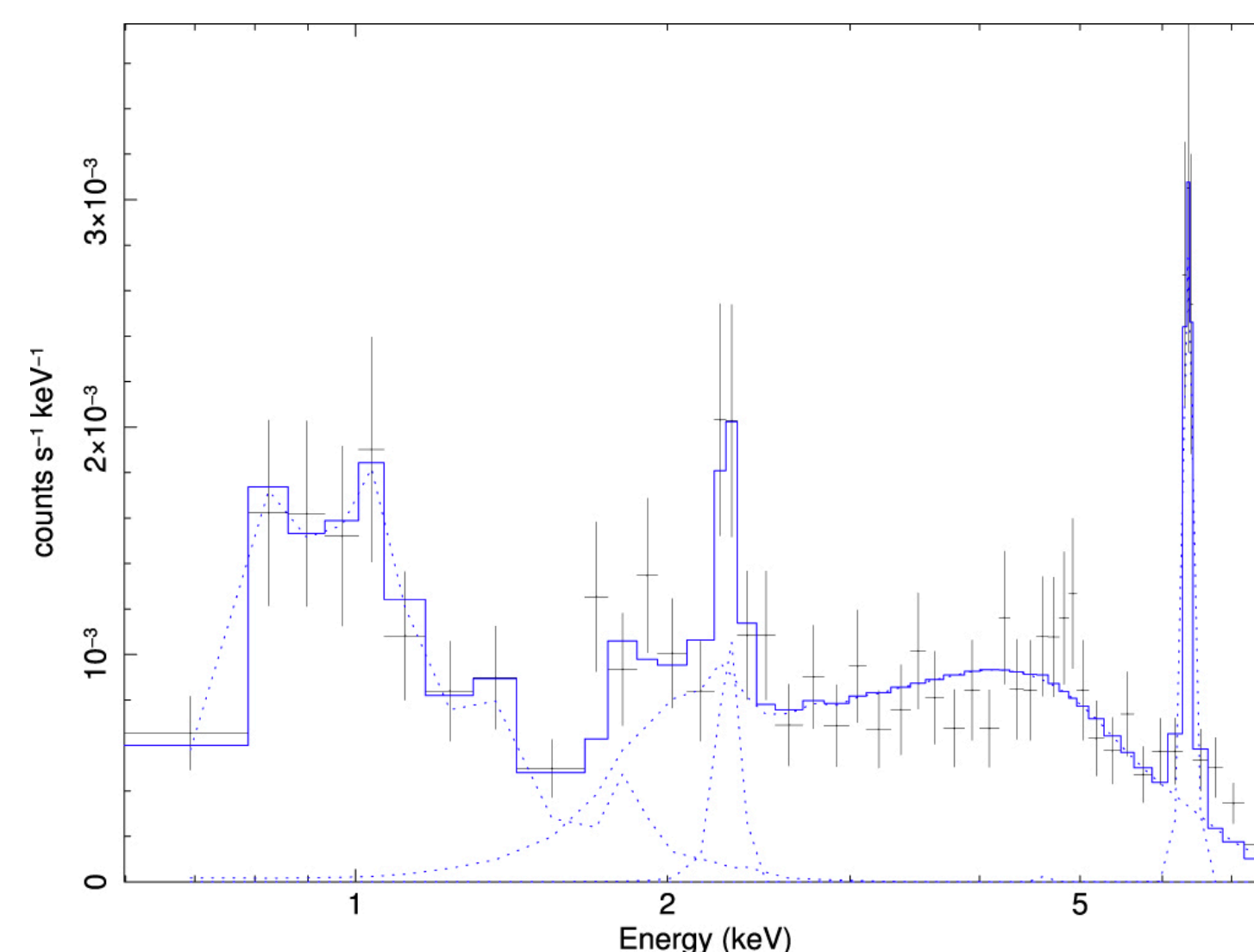
In 2010, the source was also captured by the Chandra X-ray Observatory in a historically low state, with a 2–10 keV flux of $3.6 \times 10^{-12} \text{ erg cm}^{-2} \text{ s}^{-1}$

Results



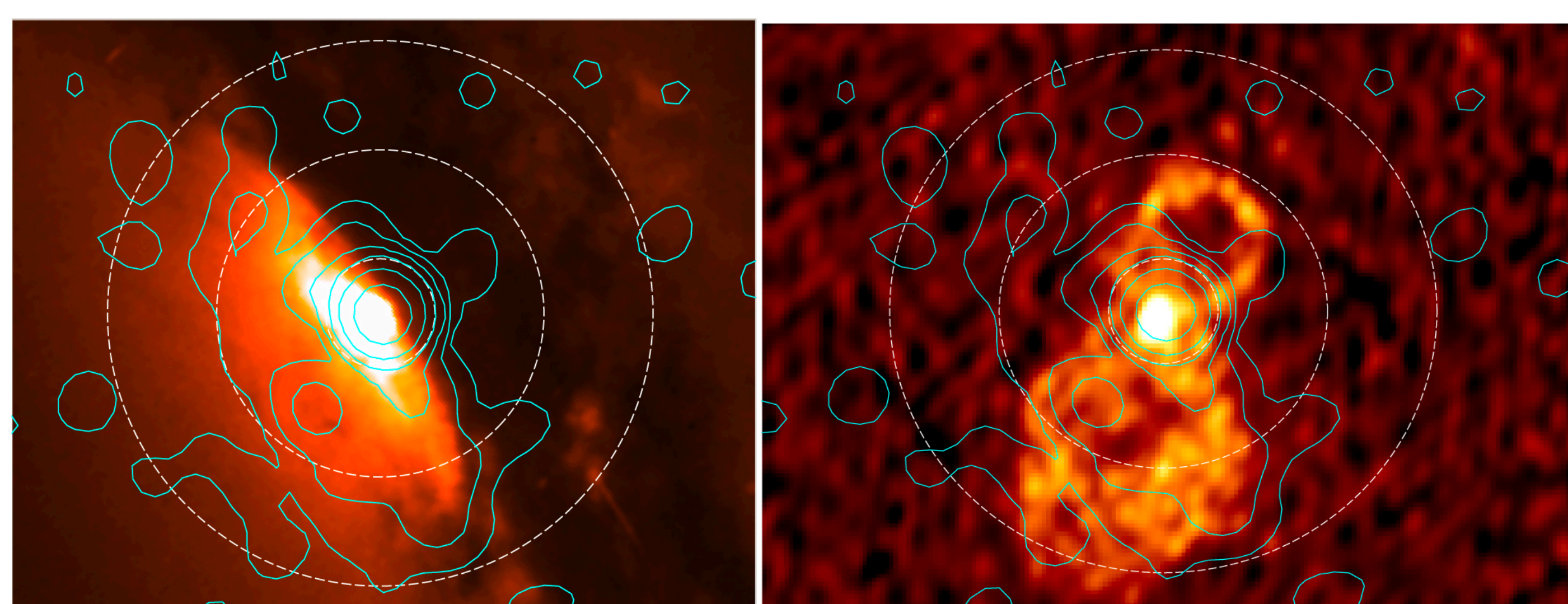
(a) Combined HETG zeroth-order image of the 0.3–2.0 keV band. (b) PSF image of the 0.3–2.0 keV band. (c) Deconvolved image of 0.3–2.0 keV with a binning factor of 0.5. (d) Combined HETG zeroth-order image of the 2.0–7.0 keV band. (e) PSF image of the 2.0–7.0 keV band. (f) Deconvolved image of 2.0–7.0 keV with a binning factor of 0.5. The inner and outer radii of the cyan annulus in all panels are 1'' and 3'', respectively.

Radial profile images of the 0.3–2.0 keV band and 2.0–7.0 keV band, respectively. Innermost points of the simulated PSF

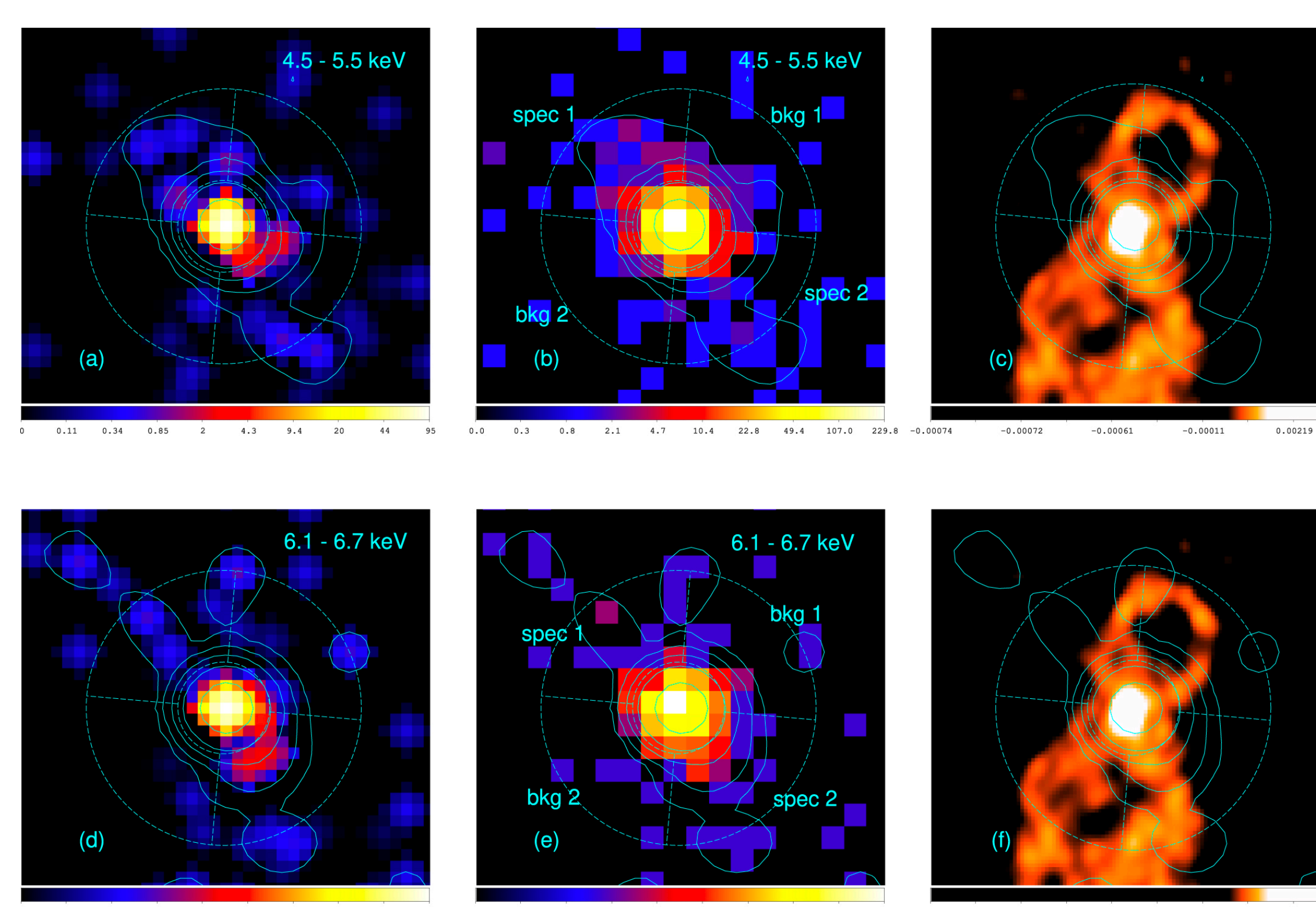


Extracted spectrum (annulus between 1'' and 3'') and parameters of the best-fit collisionally ionized model i.e., $phabs \times (apec) + phabs \times (powerlaw + zGauss + zGauss)$

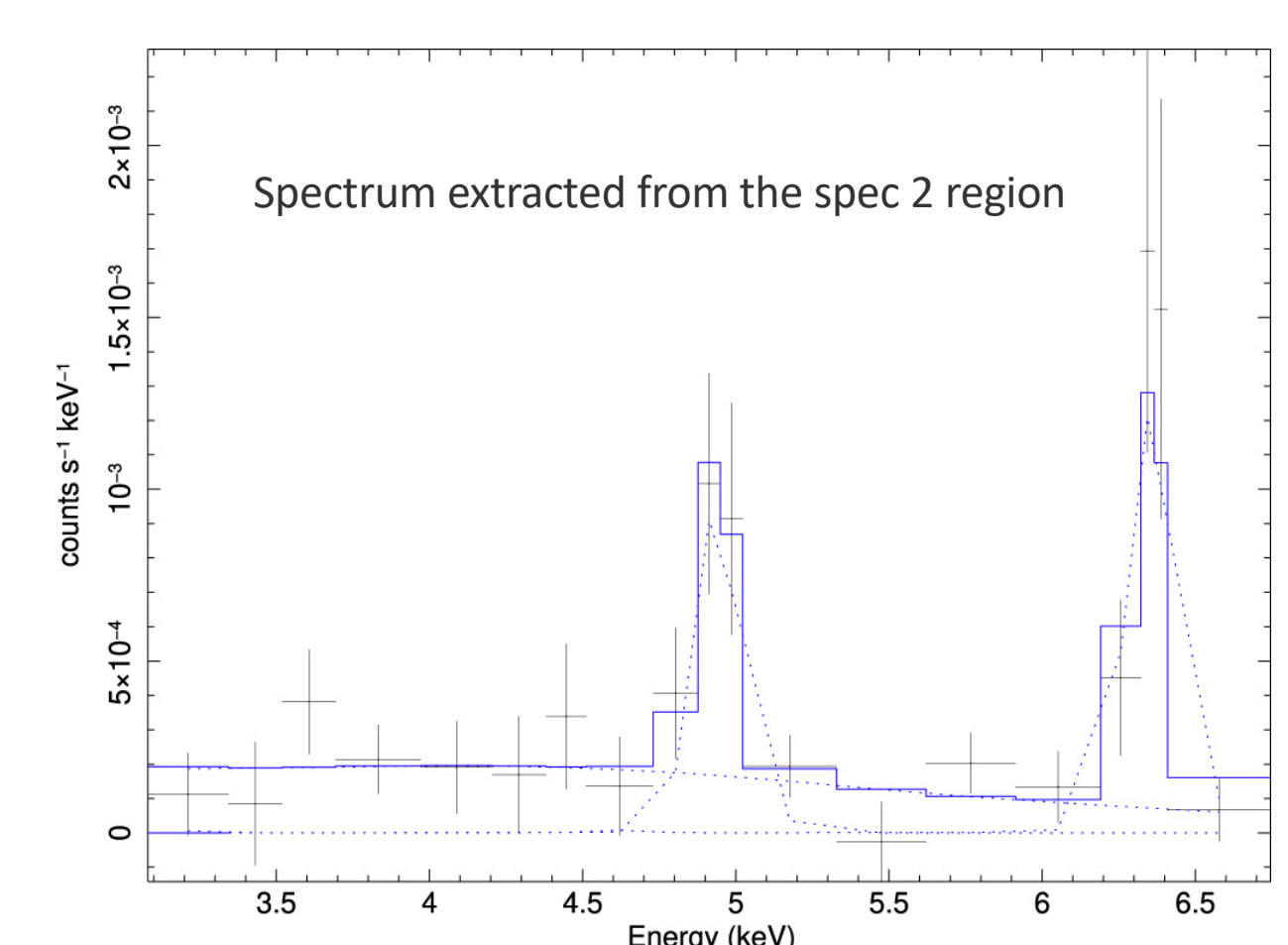
Component	Parameter	Best-fit Value
$phabs_1$	$N_{H,1} (\times 10^{22} \text{ cm}^{-2})$	$0.84^{+0.16}_{-0.16}$
$apec$	$kT \text{ (keV)}$	$0.33^{+0.21}_{-0.08}$
	Norm ($\times 10^{-4}$)	$4.66^{+8.06}_{-3.07}$
$phabs_2$	$N_{H,2} (\times 10^{22} \text{ cm}^{-2})$	$3.27^{+1.02}_{-0.53}$
$powerlaw$	Γ	1.86 (f)
	Norm ($\times 10^{-4}$)	$1.14^{+0.10}_{-0.08}$
$zGauss_1$	$E_1 \text{ (keV)}$	$2.31^{+0.02}_{-0.02}$
	Norm ($\times 10^{-6}$)	$3.98^{+2.79}_{-1.74}$
$zGauss_2$	$E_2 \text{ (keV)}$	$6.40^{+0.01}_{-0.01}$
	Norm ($\times 10^{-6}$)	$5.06^{+0.75}_{-0.75}$
***	$\chi^2/\text{d.o.f}$	32.6/41



HST/WFPC2 V-band image using the F606W filter. Overlaid are the X-ray contours of the deconvolved image in 0.3–2.0 keV band. Three white dashed circles are centered on the position of the X-ray core, which have radii of 1'', 3'', and 5'', respectively.



(a) Deconvolved image of the 4.5–5.5 keV band. (b) Combined HETG zeroth-order image of the 4.5–5.5 keV band. (c) VLA 6 cm radio image (from NED) (d) Deconvolved image of the 6.1–6.7 keV band. (e) Combined HETG zeroth-order image of the 6.1–6.7 keV band. (f) VLA 6 cm radio image



The reflected emission likely originates from material with a column density of $N_H = 9.6 \pm 2.7 \times 10^{22} \text{ cm}^{-2}$ (Middei et al. 2022). Spatially resolved extended Fe K α and the large EW in the extended region where the continuum is very weak.

Two apparent emission lines centered at energies of 4.97 and 6.39 keV were detected. The statistical significance of these two emission lines both are $\geq 99.9\%$

References

- Colbert E. J. M., Strickland D. K., Veilleux S. et al. 2005 *ApJ* **628** 113
Friedrich S., Davies R. I., Hicks E. K. S. et al. 2010 *A&A* **519** A79
Guolo-Pereira, Muryl et al. 2021 *MNRAS* **502** 3618
Marinucci A., Bianchi S., Braito V. et al. 2020 *MNRAS* **496** 3412
Middei R., Marinucci A., Braito V. et al. 2022 *MNRAS* **514** 2974
Mingozi M., Cresci G., Venturi G. et al. 2019 *A&A* **622** A146
Murphy K. D., Nowak M. A. and Marshall H. L. 2017 *ApJ* **840** 120

Contact

E-mail: jfwang@xmu.edu.cn